Available online at www.sciencedirect.com
ScienceDirect
Journal of Catalysis 243 (2006) 183–191
JOURNAL OF CATALYSIS
www.elsevier.com/locate/jcat

Synthesis and catalytic properties of a new titanosilicate molecular sieve with the structure analogous to MWW-type lamellar precursor

Weibin Fan [a], Peng Wu [b], Seitaro Namba [c], Takashi Tatsumi [a,*]

[a] *Catalytic Chemistry Division, Chemical Resources Laboratory, Tokyo Institute of Technology, 4259 Nagatsuda, Midori-ku, Yokohama 226-8503, Japan*
[b] *Shanghai Key Laboratory of Green Chemistry and Chemical Process, East China Normal University, North Zhongshan Road 3663, Shanghai 200062, People's Republic of China*
[c] *Department of Materials, Teikyo University of Science and Technology, Uenohara-machi, Yamanashi 409-0193, Japan*

Received 31 May 2006; revised 6 July 2006; accepted 9 July 2006

Abstract

A new titanosilicate molecular sieve structurally analogous to MWW-type lamellar precursors (designated as Ti-YNU-1) was postsynthesized by adjusting the titanium content in the synthesis gel and washing the as-synthesized material with acid under refluxing conditions. The samples were characterized with XRD, ICP, TG/DTA, FTIR, UV–vis, and ^{29}Si MAS NMR techniques as well as N_2, Ar, and H_2O adsorption experiments. It was indicated that compared with Ti-MWW, Ti-YUN-1 had more silanols in the structure and that its interlayer spacing was expanded by nearly 2.5 Å. In addition, the local environment of T_1 sites of the proposed structure of Ti-YNU-1 was also different from that of Ti-MWW. This led to a great increase in the pore openings connected to supercages. The formation of Ti-YNU-1 was highly dependent on the Si/Ti ratio in the synthesis gel and also might be related to the removal of about 80% templating molecules by acid treatment before calcination. Extensive evaluation of the catalytic performance of various titanosilicates for the oxidation of different cycloalkenes showed that Ti-YNU-1 behaved like a 12-membered ring (MR) zeolite. This is further confirmed by the results that a strong peak around 6.7 Å was present in the pore size distribution curve obtained from Ar adsorption for the Ti-YNU-1 sample but absent in that for the Ti-MWW sample, and that cyclohexene conversion increased but 1-hexene conversion decreased with increasing Si/Ti ratio. Compared with the other titanosilicate materials, Ti-YNU-1 showed high activity, selectivity, and stability in the liquid-phase epoxidation of bulky cycloalkenes with H_2O_2 as an oxidant. An investigation of the effect of several protic and aprotic solvents on the catalytic property of Ti-YNU-1 in the epoxidation of cyclohexene revealed that acetonitrile should be the solvent of choice considering both conversion and selectivity.

Keywords: Cycloalkene; MWW; Oxidation; Titanosilicate, YNU-1

1. Introduction

It is well known that titanosilicate catalysts exhibit high activity and selectivity in the production of oxygenated derivatives through the oxidation of hydrocarbons, alcohols, and ketones with H_2O_2 [1–7]. In particular, the MFI-type titanosilicate, TS-1, is a very efficient catalyst in the ammoximation of cyclohexanone, the liquid-phase epoxidation of propylene, and the hydroxylation of phenol to hydroquinone and catechol under mild conditions [1,3–5]. The high reactivity of the oxirane ring makes epoxides industrially important organic intermediates for producing polyurethanes, surfactants, epoxy adhesives, and corrosion-protecting agents, additives, and so on [8]. However, TS-1 is able to catalyze the oxidation only of linear alkene and smaller cycloalkene molecules, because of its limited pore openings. In contrast, large-pore Ti-Beta can serve as a catalyst in the oxidation of bulky cycloalkene molecules [7], but the rather strong hydrophilicity and the presence of Brönsted acid sites associated with framework aluminum and/or a high concentration of silanol groups at defect sites make the activity and selectivity unsatisfactorily high [9,10]. Corma et al. recently made an attempt to delaminate MWW-type materials into isolated crystalline sheets (ITQ-2) by an elaborate method [11]; then, by grafting titanocene onto the surface of ITQ-2, they prepared the titanosilicate analogue. However, the so-prepared

* Corresponding author. Fax: +81 924 5282.
E-mail address: ttatsumi@cat.res.titech.ac.jp (T. Tatsumi).

0021-9517/$ – see front matter
doi:10.1016/j.jcat.2006.07.003

material (Ti/ITQ-2) can be used with organic hydroperoxides as oxidants only under harsh conditions (i.e., in the water-free system) [12]. This is probably due to the presence of numerous hydrophilic silanols created by delamination on the exterior surface. Therefore, it is imperative to synthesize a new titanosilicate molecular sieve that not only has a larger-pore window, but also shows higher intrinsic activity and epoxide selectivity in the oxidation of bulky substrates by H_2O_2.

As we already know, MWW-type zeolite has a unique structure that contains two independent pore systems accessible via 10-MR windows. One of these systems is defined by a two-dimensional sinusoidal channel, and the other comprises supercages of $7.1 \times 7.1 \times 18.2$ Å [13]. This may provide potential opportunities for a wide variety of applications in petrochemical and fine chemical industries. Indeed, the aluminosilicate material MCM-22 is a highly selective industrialized catalyst for benzene alkylation [14], whereas the titanosilicate analogue (Ti-MWW) is not only more active than TS-1 and Ti-Beta in the liquid-phase epoxidation of linear alkenes with H_2O_2, but also highly selective for the formation of epoxides [15]. In addition, this material also shows a unique feature of selective epoxidation of the *trans*-isomer in the oxidation of *cis*- and *trans*-2-hexenes [16]. However, for the oxidation of bulky cycloalkenes, such as cyclohexene, Ti-MWW is still inferior to Ti-Beta due to the serious steric limitation imposed by its distorted 10-MR openings [7,15]. Actually, a potential advantage to the MWW structure is expected from its interlayer supercages and side pockets, which could be very useful for catalyzing the reactions involving bulky molecules. The retention of lamellar-like structure with expanded layer spacing after calcination would be an alternative way to create the open reaction space. Such a material would make the active sites within the supercages more accessible to bulky molecules. In addition, this method would also overcome the difficulties in the delamination process; the crystalline sheet structure is inevitably partially destructed, consequently affecting the catalytic performance. Hence this method would open new possibilities for applying titanosilicates in the petrochemical and fine chemical industries. In this paper, we report the preparation, characterization, and catalytic properties of such a material in the oxidation of bulky cycloalkenes.

2. Experimental

2.1. Synthesis of samples

The samples were prepared according to the postsynthesis method [17]. First, B-MWW was synthesized from fume silica, boric acid, piperidine (PI), and distilled water with a composition of SiO_2:B_2O_3:1.4PI:19H_2O. The as-prepared solid was deboronated by calcination and reflux-washing with 6 M HNO_3 aqueous solution. The highly deboronated sample was then used as a silica source to synthesize Ti-MWW lamellar precursors with the mixture comprising SiO_2:(0–0.05)TiO_2:1.4PI:(3–20)H_2O. The resultant gel was hydrothermally treated at 170 °C for 5 days under rotating conditions. Finally, the solid product was filtered, washed, dried, further treated with 2 M HNO_3, and finally calcined at 550 °C for 10 h.

2.2. Characterization of samples

The X-ray diffraction (XRD) patterns were recorded on a MAC Science M3X 1030 X-ray diffractometer with Cu$K\alpha$ radiation (40 kV, 20 mA) to identify the crystalline phase and estimate the crystallinity. The titanium coordination states of the as-synthesized and calcined materials were investigated by diffuse reflectance (DR) UV–vis spectroscopy (JASCO V-550 UV–vis spectrophotometer). Framework and OH-region infrared (IR) spectra were measured on a PE-1600 FTIR spectrometer. Before recording the spectra in the OH stretching vibration region, the samples were first evacuated at 500 °C for 2 h under high-vacuum conditions. ^{29}Si MAS NMR measurements were performed on a JEOL JNMECA 400 nuclear magnetic resonance spectrometer at ambient temperature. The chemical shift was referenced to an external standard of polydimethylsilane. The spinning rate of the rotor was 5.0 KHz. A pulse length of 7 μs and the corresponding angle of 90° were applied, and about 3000 scans were accumulated with a repetition time of 30 s. The spectra were deconvolved with the Gaussian–Lorentzian mixed equation. N_2 adsorption at −196 °C and H_2O adsorption at 25 °C were carried out on Belsorp 28SCA and Belsorp 18SCA instruments, respectively, and Ar adsorption at −186 °C was performed on a Quantachrome Autosorb-1 instrument. Before measurement, the sample was first pretreated at 300 °C for 2 h under high-vacuum conditions. TG/DTA was measured on an ULVAC-Riko TGD 9600 thermal analysis system. The temperature was ramped to 1000 °C at a heating rate of 10 °C min^{-1}. The chemical composition of the samples was determined by inductively coupled plasma–atomic emission spectrometry (Shimadzu ICPS-8000E).

2.3. Catalytic measurements

The liquid-phase oxidation of alkenes with H_2O_2 (31% in aqueous solution) was carried out at 60 °C for 2 h in a round-bottom flask equipped with a condenser under stirring conditions. The temperature was controlled with a water bath. Unless specified otherwise, the reaction mixture was as follows: 0.05 g of catalyst, 10 ml of acetonitrile as solvent, 10 mmol of alkene as substrate, and 10 mmol of H_2O_2 as oxidant. The product was analyzed on a Shimadzu GC-14B gas chromatograph equipped with a 50-m OV-1 capillary column and a flame ionization detector. The amount of the unconverted H_2O_2 was determined by titrating with 0.1 M $Ce(SO_4)_2$ aqueous solution.

3. Results and discussion

3.1. Synthesis and characterization of Ti-YNU-1

XRD measurements showed that, using the postsynthesis method and washing the as-synthesized Ti-MWW lamellar precursor with acid under reflux conditions before calcination, the expanded layer structure was retained even after calcination [18]. This prepared material has been denoted Ti-YNU-1. The reason for formation of the expanded layer structure remains unclear, although we found that this formation was

closely related to the Si/Ti ratio in the synthesis gel. Fig. 1 shows that the higher the Si/Ti ratio, the more the expanded layer structure was retained after acid treatment and calcination. However, when the Si/Ti ratio was lowered to 50, the expanded layer structure disappeared, and the MWW structure was formed. In addition, the formation of Ti-YNU-1 structure might be also related to the degree of removal of the residual B ions and templating molecules; it was found that almost all of the B ions and about 80% of the templating molecules occluded in the channels were removed by the acid treatment, as indicated by the ICP analysis results (not shown) and the TG measurements (Fig. 2), respectively. This is supported by the fact that Ti-YNU-1 could not be obtained by the direct hydrothermal synthesis method irrespective of the Si/Ti ratio in the synthesis gel (not shown here).

Table 1 gives the XRD data and unit-cell parameters, estimated by assuming hexagonal symmetry from the 101 and 102 diffraction lines. Both of these lines were very intense, thus making it easy to accurately determine their positions or d values. At present, there are two space groups of hexagonal P6/mmm and orthorhombic Cmmm for the proposed MWW structure. The orthorhombic Cmmm structure is energetically favored over the hexagonal P6/mmm structure, as confirmed by the ^{29}Si MAS NMR of dealuminated MCM-22 [19]. However, we still use the hexagonal model to calculate the unit-cell parameters, because there is no substantial difference with respect to the basic topology of the framework [20]. Moreover, to date no standard diffraction planar indexes (hkl) have been reported for the orthorhombic structure; thus, acquiring its exact unit-cell parameters is very difficult. Compared with Ti-MWW, the diffraction lines associated with c-axis direction of Ti-YNU-1 all shifted to low 2θ positions (Table 1). This is indicative of the larger unit-cell parameter c. Indeed, Table 1 shows that the parameter c increased from 24.98 to 27.47 Å. Because the crystalline structure within layers is highly rigid, it is reasonable to envisage that the increase in c is due mainly to the enlarged interlayer spacing. Indeed, a and b values of two samples were highly similar. Thus, it can be inferred that the interlayer spacing of Ti-YNU-1 is greater than that of Ti-MWW and its lamellar precursor by about 2.5 and 0.8 Å, respectively. This implies

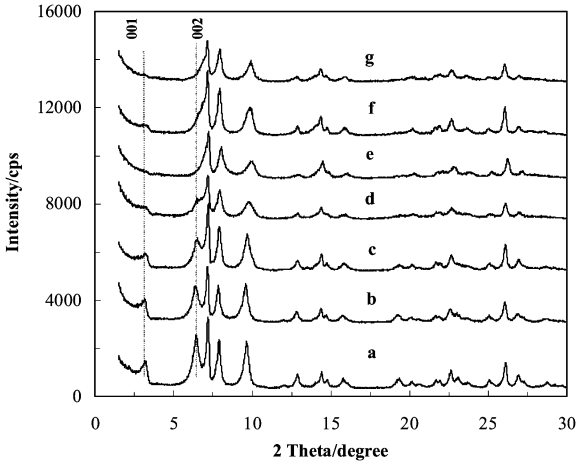

Fig. 1. XRD patterns of the materials prepared by acid treating and subsequently calcining the Ti-MWW lamellar precursors synthesized with a synthesis gel having a Si/Ti ratio of (a) 100, (b) 85, (c) 70, (d) 60 (e) 50, (f) 40, and (g) 30.

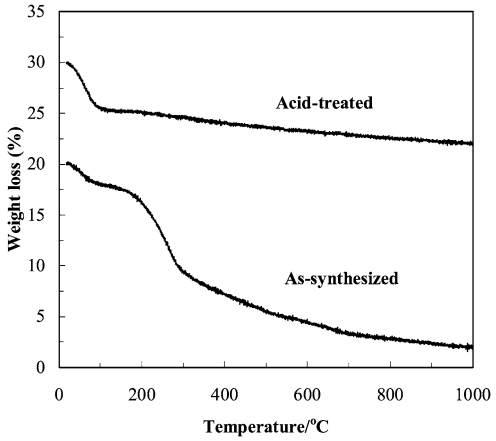

Fig. 2. TG curves of the as-synthesized Ti-MWW lamellar precursor (Si/Ti = 106) and the acid-treated sample (Si/Ti = 240).

Table 1
XRD data and unit-cell parameters of the as-synthesized lamellar precursor (Si/Ti = 106), Ti-MWW (Si/Ti = 106), and Ti-YNU-1 (Si/Ti = 240)

Sample hkl	As-synthesized		Ti-MWW (calcined)		Ti-YNU-1	
	2θ	d (Å)	2θ	d (Å)	2θ	d (Å)
001	3.28	26.92	3.50	25.22	3.20	27.59
002	6.60	13.38	7.14	12.37	6.46	13.67
100	7.22	12.23	7.14	12.37	7.18	12.30
101	7.94	11.13	8.02	11.01	7.86	11.24
102	9.80	9.02	10.10	8.75	9.64	9.17
004	–	–	14.22	6.22	13.98	6.33
302	22.76	3.90	22.84	3.89	22.62	3.93
310	26.26	3.39	26.14	3.41	26.10	3.41
Unit-cell parameters[a]	$a = 14.15$ Å $b = 14.15$ Å $c = 26.69$ Å $V = 4626.38$ Å^3 $\alpha = \beta = 90°$ $\gamma = 120°$		$a = 14.19$ Å $b = 14.19$ Å $c = 24.98$ Å $V = 4352.85$ Å^3 $\alpha = \beta = 90°$ $\gamma = 120°$		$a = 14.24$ Å $b = 14.24$ Å $c = 27.47$ Å $V = 4821.37$ Å^3 $\alpha = \beta = 90°$ $\gamma = 120°$	

[a] The unit-cell parameters were determined in terms of hexagonal model from 101 and 102 diffraction lines.

that the pore windows of supercages are significantly expanded, making it possible to accommodate the substrates with large molecule sizes.

The edge-on TEM lattice images of thin platelike crystallites of Ti-YNU-1 and Ti-MWW show that the layer spacing of Ti-YNU-1 was greater than that of Ti-MWW and that the interlayer spacing of Ti-YNU-1 was increased by about 2.5 Å [18,21], in good agreement with the XRD characterization. The TEM characterization also shows that Ti-YNU-1 differs greatly from ITQ-2, which consists of separate sheets [11]. In contrast, Ti-YNU-1 completely retains the three-dimensional feature of Ti-MWW but with a significantly expanded interlayer spacing, as recently found by Ruan and co-workers by HRTEM [21]. This finding is also strongly supported by the XRD characterization. The diffraction lines of ITQ-2 is very weak in intensity and almost indiscernible as a result of lack of long-range order along the *c*-axis, [11] whereas those of Ti-YNU-1 are similar to those of Ti-MWW.

N_2 adsorption/desorption isotherms of Ti-YNU-1, like Ti-MWW, displayed adsorption behavior typical of microporous materials, with an external surface area of 61.4 $m^2\,g^{-1}$ (not shown here for brevity). This provides more evidence that of the zeolitic structure of Ti-YNU-1. Ti-YNU-1 has a much greater adsorption capacity than Ti-MWW. The surface areas and pore volumes, calculated by the Langmuir and *t* methods respectively, are about 676 $m^2\,g^{-1}$ and 0.202 $ml\,g^{-1}$ for Ti-YNU-1 and 528 $m^2\,g^{-1}$ and 0.154 $ml\,g^{-1}$ for Ti-MWW. This supports the substantial expansion of the interlayer spacing.

Ruan et al. suggested that Ti-YNU-1 was formed possibly by pillaring the crystalline sheets with silicate species [21]. However, some important findings remain unexplained. Ti content in the framework strongly affected the formed products, although Ti cations probably selectively occupy some certain lattice sites, and Ti-YNU-1 could not be formed by the direct hydrothermal synthesis method even when the same acid-treating procedures were used for the as-synthesized sample with very low Ti content (e.g., a Si/Ti ratio of 120). In addition, to the best of our knowledge, there are no reports indicating that pillaring of crystalline sheets, such as clay, with silicates or metallonate species could occur in such a severe acid-treating condition (2 M HNO_3, reflux), because this would deteriorate the structure of crystallite sheets [22,23]. Almost all pillaring processes were carried out under basic or mildly acidic conditions. Therefore, the exact linkage between the layers after removing the templating molecules remains unresolved. Further studies on the formation mechanism and the corresponding structure simulation will be reported elsewhere [24].

IR spectra of Ti-YNU-1 and Ti-MWW were similar in terms of the shape and band positions characteristic of framework vibrations; however, a substantial difference can be seen in the OH– stretching vibration region (Fig. 3). Compared with Ti-MWW sample, Ti-YNU-1 showed a much more intense band at 3728 cm^{-1}, probably ascribed to internal hydroxyl-bonded silanols [25], with the other three bands attributed to external (terminal) Si–OH (3738 cm^{-1}), vicinal silanols (3690 cm^{-1}), and silanol nests (3500 cm^{-1}) were almost the same [25,26]. This shows that more silanol groups were present in the Ti-YNU-1 sample. This would result mainly from the different structures of T sites situated in interlayer surface, because the as-synthesized sample contains only a small amount of B atoms (Si/B > 200), making it unlikely that much more B-deficient defect sites are present in Ti-YNU-1 than in Ti-MWW as a result of the acid treatment. The greater amount of silanols in Ti-YNU-1 was also confirmed by ^{29}Si MASNMR spectroscopy (Fig. 4). A signal at 88.6 ppm, assigned to $SiO_2(OH)_2(Q^2)$ and/or possibly $Si(OH)(OTi)(OSi)_2$, appeared in the spectrum of Ti-YNU-1, whereas it was absent in Ti-MWW. Fig. 5 shows

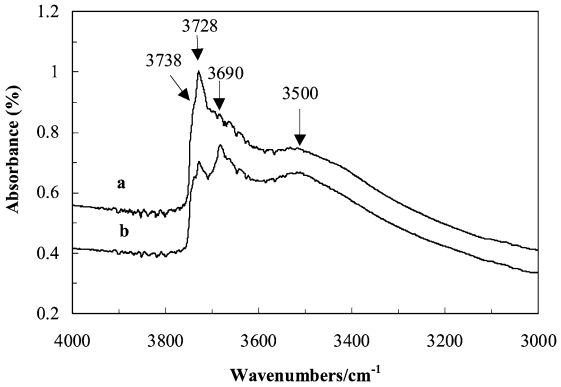

Fig. 3. FTIR spectra of (a) Ti-YNU-1 (Si/Ti = 240) and (b) Ti-MWW (Si/Ti = 40) in hydroxyl stretching region.

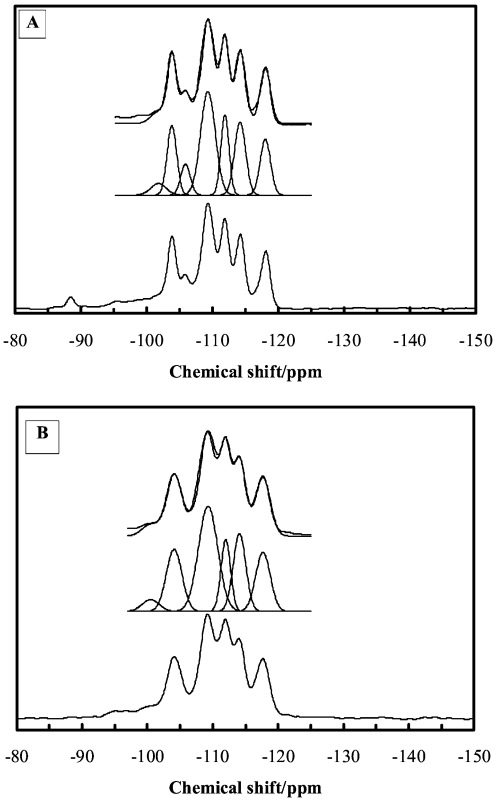

Fig. 4. Experimentally recorded ^{29}Si MASNMR spectra of (A) Ti-YNU-1 (Si/Ti = 240) and (B) Ti-MWW (Si/Ti = 40) in the range from −150 to −80 ppm are shown on the bottom. The deconvoluted components between −97 and −125 ppm are depicted in the middle; the superposition of the simulated and the experimentally recorded spectra are shown on the top.

that the amount of the adsorbed water on Ti-YNU-1 was about four-fold that on Ti-MWW, demonstrating that Ti-YNU-1 is more hydrophilic than Ti-MWW. This also proves that Ti-YNU-1 has significantly more silanol groups than Ti-MWW.

It has been reported that MWW-type materials have at least eight crystallographically inequivalent T sites [13]; this has been supported by ^{29}Si MAS NMR spectroscopy [19]. According to the proposed structure, the hexagonal model has eight distinct sites with a framework occupancy ratio of 1:3:3:1:1:3:3:3, whereas the orthorhombic form has 13 sites with a multiplicity ratio of 1:1:1:1:2:2:1:1:2:2:1:1:2. The spectrum of Ti-MWW matches well with those reported in Refs. [20,27]; five lines were observed (Fig. 4B), suggesting several distinctive crystallographic sites in Ti-MWW with overlapping resonances. In contrast, six resolved lines characteristic of Q^4 sites appeared in the spectrum of Ti-YNU-1 (Fig. 4A). Table 2 gives the deconvolution data for the ^{29}Si MAS NMR spectra of Ti-YNU-1 and Ti-MWW, along with the possible signal assignments. The relative intensities of the resonances of Ti-YNU-1 and Ti-MWW are approximately 3:1:6:3:3:2 and 3:8:2:3:2, respectively. Although the NMR data of Ti-YNU-1 are consistent with both the hexagonal model [3:1:(3 + 3):3:3:(1 + 1) for T_2:T_1:(T_3 + T_8):T_7:T_6:(T_4 + T_5), respectively] and the orthorhombic form [(2 + 1):1:(1 + 1 + 2 + 2):(2 + 1):(1 + 2):(1 + 1) for (T_2 + T_6):T_1:(T_3 + T_4+ T_5 + T_{13}):(T_{10} + T_{12}):(T_7 + T_9):(T_8 + T_{11}), respectively], in light of the probability of line overlap or degeneracy, we may conclude that the NMR line intensities of Ti-MWW support the orthorhombic structure. Therefore, Table 2 provides the plausible signal assignments according to the orthorhombic model to allow ready comparison of the local environments of various T sites between these two materials. Fig. 4 shows that the signal attributed to T_1 sites can be clearly resolved into a separate line for Ti-YNU-1, and the average T–O–T angle is estimated as 140.9° according to the Engelhardt–Radeglia equation [28]. In contrast, this line was overlapped with the others in the spectrum of Ti-MWW. This indicates that the local environment of T_1 sites of Ti-MWW matched well with the proposed orthorhombic structure, which has an average T–O–T angle of 147.5° at T_1 sites. Although these assignments are not definitive (the definitive assignments require two-dimensional NMR experiments to establish Si–O–Si connectivity), and hence should be used only in a qualitative sense, the significant difference in average T–O–T angle at T_1 sites between two samples could be considered evidence that Ti-YNU-1 has a layered structure different from that of Ti-MWW- or MWW-type materials.

The diffuse reflectance UV–vis spectroscopy (Fig. 6) shows that like Ti-MWW, all Ti atoms in Ti-YNU-1 have a tetrahedral coordination, as evidenced by the presence of only one band around 210 nm but no bands above 250 nm due to oc-

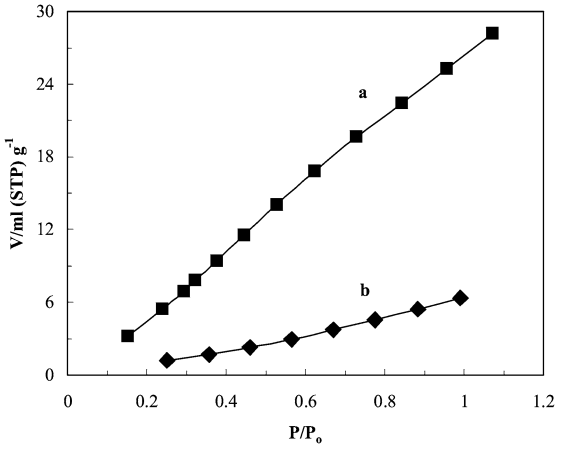

Fig. 5. H_2O adsorption isotherms at 25 °C of (a) Ti-YNU-1 (Si/Ti = 240) and (b) Ti-MWW (Si/Ti = 40).

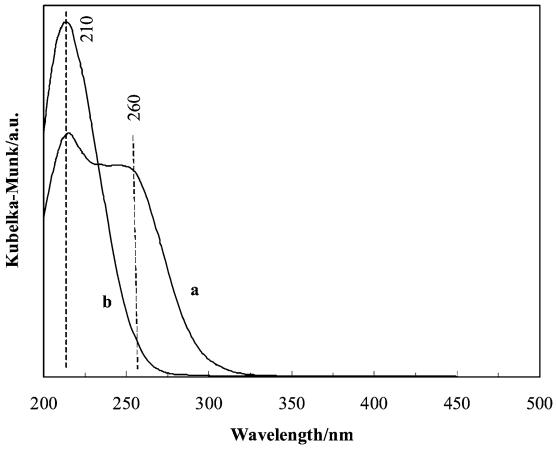

Fig. 6. Diffuse reflectance UV–vis spectra of the (a) as-synthesized lamellar precursor (Si/Ti = 106) and (b) Ti-YNU-1 (Si/Ti = 240).

Table 2
Deconvolution data of ^{29}Si MAS NMR spectra of Ti-YNU-1 (Si/Ti = 240) and Ti-MWW (Si/Ti = 40) and tentative signal assignments

Ti-YNU-1				Ti-MWW			
Chemical shift	Average T–O–T angle (°)[a]	Relative area	Assignment[b]	Chemical shift	Average T–O–T angle (°)[a]	Relative area	Assignment[b]
−103.83	137.5	3	$T_2 + T_6$	−105.01	139.4	3	$T_2 + T_6$
−105.94	140.9	1	T_1	−110.75	148.7	8	$T_1 + T_3 + T_4 + T_5 + T_{12} + T_{13}$
−109.31	146.4	6	$T_3 + T_4 + T_5 + T_{13}$	−112.99	152.3	2	T_{10}
−111.89	150.5	3	$T_{10} + T_{12}$	−115.38	156.2	3	$T_7 + T_9$
−114.24	154.3	3	$T_7 + T_9$	−119.02	162.1	2	$T_8 + T_{11}$
−118.03	160.5	2	$T_8 + T_{11}$				

[a] Average T–O–T angle is calculated according to Engelhardt and Radeglia equation.
[b] Peak assignments are tentative and based on the observed peak intensities, spin-lattice relaxation time behavior, and a qualitative correlation between ^{29}Si chemical shifts and T–O–T angles.

tahedrally coordinated Ti or titanium oxides [29]. In contrast, an additional band at about 260 nm, arising mainly from octahedral Ti species located in the interlayer region, was observed for the as-synthesized Ti-MWW lamellar precursor. However, these extra-framework Ti species in the as-synthesized sample were selectively removed by acid treatment. Framework incorporation of Ti is also indicated by the presence of two absorption bands at about 930 and 960 cm^{-1} in the IR spectra. This is attributed to the stretching vibration of Si–O–Ti bonds, where Ti atoms are located at crystallographically inequivalent lattice sites with different T–O bond lengths [30]. For Ti/ITQ-2, the grafted Ti is merely located at the external surface but not at the truly isomorphously substituted lattice sites. Therefore, the Ti species should be similar to those of Ti-MCM-41 prepared via the grafting method [31]. This probably accounts for the fact that the epoxidation of cyclohexene over Ti/ITQ-2 can be carried out only in the absence of water [11].

3.2. Catalytic properties of Ti-YNU-1

3.2.1. Catalytic properties of Ti-YNU-1 in the liquid-phase oxidation of alkenes

Fig. 7 shows the relationship between the conversion of Ti-YNU-1 and its Ti contents for the oxidation of cyclohexene and 1-hexene. It is clear that with increasing Ti content, the 1-hexene conversion increased monotonously, whereas cyclohexene conversion showed a reverse relationship. This result is consistent with the findings presented above. As the Si/Ti ratio in the synthesis gel decreased, the expanded layer structure of Ti-YNU-1 gradually disappeared, and Ti-MWW was formed. The molecules of linear 1-hexene are small enough to enter into both the interlayer and intralayer 10-MR openings of Ti-MWW and access all of the active sites. As a result, the more tetrahedral Ti sites in the sample, the higher the catalytic activity. In contrast, cyclohexene with a larger kinetic diameter hardly penetrates the rather distorted 10-MR pore windows. Thus, for Ti-MWW, only the Ti sites on the external surface and

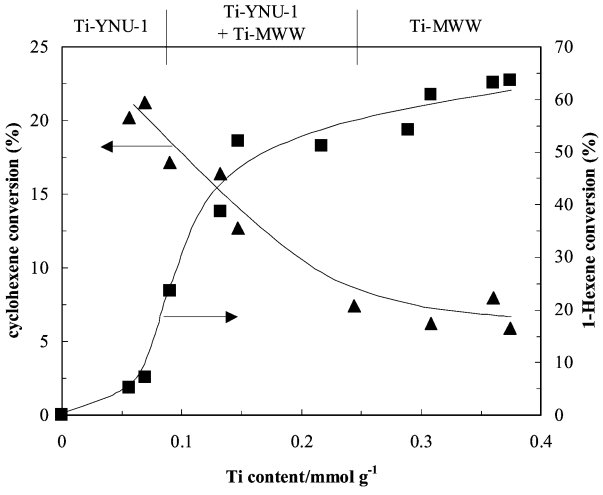

Fig. 7. Effect of titanium content on the catalytic activity of Ti-YNU-1 and Ti-MWW. (Reaction conditions: 0.05 g catalyst, 10 mmol substrate, 10 mmol H_2O_2 (31% in aqueous solution), 10 ml acetonitrile, 60 °C, 2 h.)

side pockets act as active sites for the oxidation of cyclohexene. Actually, the Ti sites in the supercages of Ti-MWW have potential for the oxidation of bulky molecules, but the entrance of bulky molecules into the supercages is seriously restricted by 10-MR pore windows. Because the two-dimensional intralayer sinusoidal channels are independent of the supercages, expanding the interlayer space is the most effective way to make the Ti sites in the supercages serve as active sites for oxidizing bulky substrate molecules. As described above, the higher the Si/Ti ratio, the more the expanded layer structure is retained even after calcination, and consequently the greater the accessibility of the Ti sites to cyclohexene molecules, resulting in enhanced activity with decreasing Ti content.

3.2.2. Comparison of the catalytic property of Ti-YNU-1 with other typical titanosilicate molecular sieves for the oxidation of cyclohexene

Table 3 summarizes the catalytic results for the oxidation of cyclohexene over various titanosilicate molecular sieves. Compared with Ti-YNU-1, large-pore Ti-Beta not only exhibited lower activity, but also gave much lower epoxide and H_2O_2 selectivity, whereas it is known to be an effective catalyst for the oxidation of bulky molecules. In fact, the presence of acid sites, originating from numerous defect sites [10] in Ti-Beta, is a severe drawback for the oxidation reactions involving multielementary steps, making it very difficult to obtain high selectivity for the desired product. In the case of cyclohexene oxidation, the substrate undergoes both allylic oxidation and epoxidation, followed by nucleophilic ring opening of epoxide. The relatively high acidity of Ti-Beta enhances the hydrolysis of the oxirane ring, resulting in the production of more diol at the expense of epoxide [9,10]. Ti-MWW exhibited moderate cyclohexene conversion, whereas TS-1 and Ti-mordenite (MOR) were less effective for the oxidation of this substrate. Although Ti-MWW, like TS-1, has 10-MR pore openings, which prevent the substrate molecules from accessing the active sites within the channels, the 12-MR side pockets on the exterior surface led to the high activity, compared with TS-1. As for Ti-MOR, the lower activity was perhaps due to the weak oxidative ability of Ti sites as a result of the different structure, the preparation method (postsynthesis using $TiCl_4$), and/or a diffusion problem caused by its one-dimensional channels.

3.2.3. Oxidation of different cycloalkenes over various titanosilicate molecular sieves

The turnover number (TON) for the oxidation of different cycloalkenes over various titanosilicates is depicted in Fig. 8. Ti-YNU-1 exhibited much higher oxidation activity than other materials, as evidenced by showing the much higher TON. Although TS-1 gave a high conversion for the oxidation of cyclopentene, its activity drastically decreased when oxidizing cyclohexene and decreased more severely with increasing size of cycloalkene molecules due to increasing steric restrictions. Ti sites in Ti-MWW have been reported to have much stronger intrinsic ability than those in TS-1 for the oxidation of linear alkenes [15], but it exhibited an obviously low conversion in the oxidation of cyclopentene compared with TS-1. This shows

Table 3
Cyclohexene oxidation over various titanosilicate molecular sieves with acetonitrile as a solvent[a]

Molecular sieve	Si/Ti	Conv. (%)	Selectivity (%)			H_2O_2	
			Epoxide	Diol	Others[b]	Conv. (%)	Selec. (%)
TS-1	83	3.3	17.9	75.7	6.4	–	–
3D Ti-MWW	45	8.1	35.0	58.8	6.2	10.6	74.8
Ti-MOR[c]	92	9.0	55.0	39.1	5.9	14.3	63.5
Ti-Beta	35	16.5	78.4	18.6	3.0	32.3	51.6
Ti-YNU-1	240	21.2	90.8	3.5	5.8	26.2	78.5

[a] Reaction conditions: 0.05 g catalyst, 10 mmol substrate, 10 mmol H_2O_2 (31% in aqueous solution), 10 ml acetonitrile, 60 °C, 2 h.
[b] 2-Cyclohexene-1-ol and 2-cyclohexene-1-one.
[c] It was post-prepared by treating the dealuminated sample (Si/Al = 468) with $TiCl_4$ vapor at 500 °C for 1 h. The reaction conditions are the same as that used for other titanosilicates with the exception of using 0.2 g catalyst.

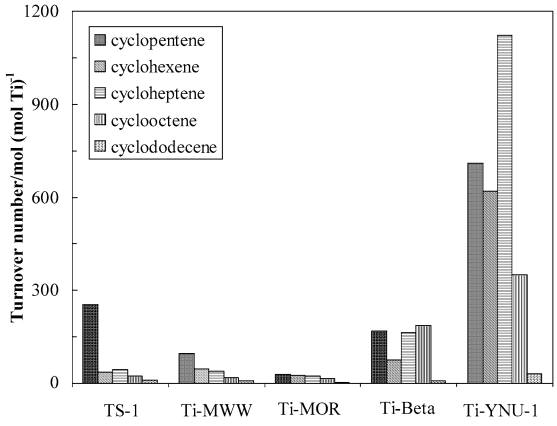

Fig. 8. Turnover number for the oxidation of different clycloalkenes over various titanosilicates. (Reaction conditions: 0.05 g catalyst, 10 mmol substrate, 10 mmol H_2O_2 (31% in aqueous solution), 10 ml acetonitrile, 60 °C, 2 h.)

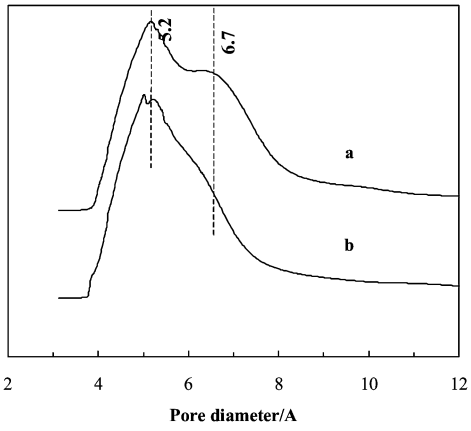

Fig. 9. Pore size distribution curves of (a) Ti-YNU-1 (Si/Ti = 240) and (b) Ti-MWW (Si/Ti = 40) obtained from argon adsorption at −186 °C.

that greater steric restriction is imposed on Ti-MWW, indicating that the 10-MR opening of Ti-MWW is rather distorted and smaller than that of TS-1. In contrast, the catalytic activity of Ti-YNU-1 and Ti-Beta initially increased sharply up to C_7 or C_8 cycloalkenes (except for the low conversion of cyclohexene), and then drastically declined. It can be deduced that the drastic decrease in cyclooctene conversion of Ti-YNU-1 resulted from the steric hindrance. The fact that for Ti-Beta, the conversion was highest for cyclooctene among the various cycloalkenes suggests that the interlayer pore window of Ti-YNU-1 is slightly smaller than that of Ti-Beta.

Because of the low activity, it is impossible for us to precisely estimate the effective pore size of Ti-MOR from the cycloalkene oxidation reactions for the moment, but it can be seen that the conversion gradually declined as cycloalkene molecules increased in size. It is reasonable to conceive that Ti-MOR has a smaller pore size than Ti-YNU-1 but larger than that of TS-1, because the conversion of cyclopentene on Ti-MOR (10.2%) was similar to that of cyclohexene (9.0%) but higher than that of cycloheptene (7.5%). This is indicative of the steric constraints when using Ti-MOR to catalyze the oxidation of cycloheptene. Thus, it is conceivable that the average pore size of various titanosilicates decreased in the order Ti-Beta > Ti-YNU-1 > Ti-MOR > TS-1 > Ti-MWW. This result is consistent with the XRD and TEM characterization that the interlayer spacing of Ti-YNU-1 was increased by about 2.5 Å compared with Ti-MWW, because the effective pore openings of Beta and MOR zeolites were 7.1 × 7.3 and 7.0 × 6.5 Å, respectively, whereas that of MWW between layers was 4.0 × 5.5 Å [32]. Thus, it could be inferred that the interlayer pore window of Ti-YNU-1 should be about 6.5 Å. Ar adsorption measurement confirmed that a strong peak around 6.7 Å was present in the curve of pore size distribution for the Ti-YNU-1 sample, whereas it was absent for the Ti-MWW material (Fig. 9).

3.2.4. *Effect of solvent on the catalytic performance of Ti-YNU-1*

It is known that solvent has a strong effect on the catalytic performance of metallosilicate molecular sieves [2,33,34]. Methanol as a solvent favors the oxidation of alkenes and alcohols by H_2O_2 over TS-1 due to the hydrophobicity of the catalyst [2–5,35], whereas relatively hydrophilic Ti-Beta shows high catalytic activity when acetonitrile is used as a solvent [37]. Thus, two types of species have been proposed to account for the favorable effect of solvents. Species I elucidates the primary role of protic solvents, whereas species II is the active intermediate in the presence of aprotic solvent together with water. Furthermore, the polarity and geometry of the solvent, as well as its possible interaction with the active sites, also probably cause the significant difference [34]. The influence of the nature of solvents on the catalytic performance of Ti-YNU-1 for the oxidation of cyclohexene is presented in Table 4. As in the hydrothermally synthesized Ti-Beta, acetoni-

Table 4
Catalytic results of Ti-YNU-1 (Si/Ti = 240) for the oxidation of cyclohexene in different solvents[a]

Solvent	Dielectric constant	Conv. (%)	Selectivity (%)			H_2O_2	
			Epoxide	Diol	Others[b]	Conv. (%)	Selec. (%)
Acetonitrile (A)	37.5	21.2	90.8	3.5	5.8	26.1	78.5
Acetone (A)	20.7	13.0	76.4	20.2	3.4	21.6	60.9
Methyl ethyl ketone (A)	18.5	11.2	69.0	26.1	5.0	17.1	67.1
Methanol (P)	32.7	18.4	11.7	13.4	74.9	19.5	96.1
Ethanol (P)	24.5	18.5	51.6	25.1	23.3	26.3	88.6
t-Butyl alcohol (P)	10.9	4.8	59.4	38.0	2.6	8.6	57.0

[a] Reaction conditions: 0.05 g catalyst, 10 mmol substrate, 10 mmol H_2O_2 (31% in aqueous solution), 10 ml acetonitrile, 60 °C, 2 h.
[b] 2-Cyclohexene-1-ol, 2-cyclohexene-1-one and glycol methyl ethers.

trile as a solvent not only promoted cyclohexene conversion, but also greatly enhanced epoxide selectivity. In contrast, use of the protic solvent of methanol resulted in the solvolysis of the once formed epoxide to produce glycol methyl ethers. This is different from Ti-Beta synthesized by the dry-gel method [36] and TS-1. This can be interpreted in terms of the relatively high hydrophilicity of Ti-YNU-1, leading to the easy formation of species II.

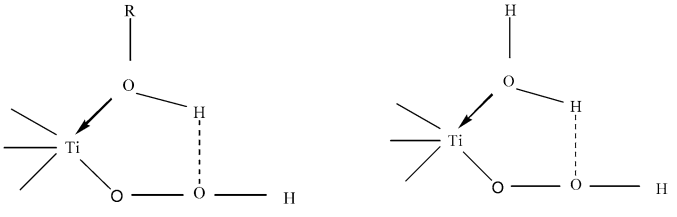

Species I **Species II**

Furthermore, basic acetonitrile molecule could also poison the acid sites. Among protic solvents, compared with methanol and ethanol, *t*-butyl alcohol led to a low activity, which could be attributed to the decreased electrophilicity of species I and the serious steric constraints on its formation [6]. This is accompanied by the remarkable increase in epoxide selectivity and a sharp decline in glycohol alkyl ethers. The influence of the aprotic solvents with different polarities on the catalytic behavior of Ti-YNU-1 was also similar to that on Ti-Beta; that is, the activity decreased in the sequence MeCN > MeCOMe > MeCOEt [34]. This was ascribed to the increase in substrate concentration around Ti centers with increasing polarity [34]. In addition, more diol was generated at the expense of the epoxide due to the decreased basicity. Considering both activity and selectivity, acetonitrile is the solvent of choice.

3.2.5. *Catalytic stability of Ti-YNU-1*

The catalytic stability of Ti-YNU-1 was further investigated using cyclohexene oxidation as a model reaction. The reaction conditions for the repeated runs were as follows: the reaction temperature of 60 °C, the reaction time of 2 h, cyclohexene/H_2O_2 = 1/1 (mol mol^{-1}), MeCN/cyclohexene = 1/1 (ml mmol^{-1}), and catalyst/cyclohexene = 1/100 (g mmol^{-1}). After each run, the catalyst was washed with acetone and then distilled water four times. The solid material was dried at 100 °C and then calcined at 550 °C for 8 h before the next run. Fig. 10 depicts the catalytic results of eight

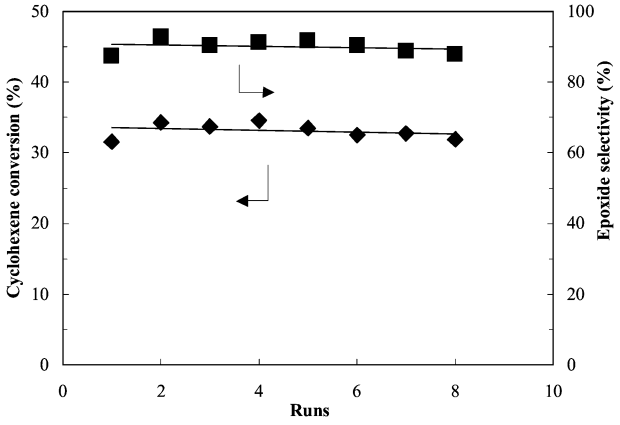

Fig. 10. Catalytic results of Ti-YNU-1 (Si/Ti = 240) in the oxidation of cyclohexene for eight repeated runs with regeneration.

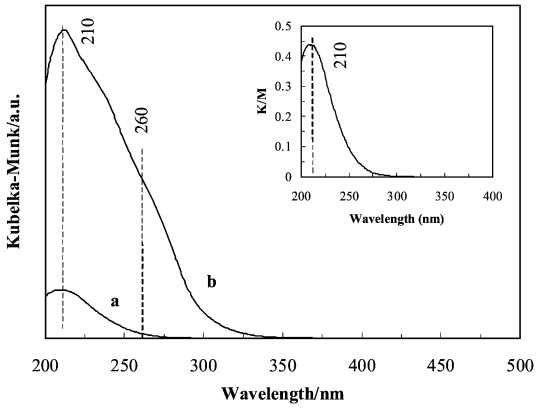

Fig. 11. Diffuse reflectance UV–vis spectra of (a) Ti-YNU-1 (Si/Ti = 221) and (b) Ti-Beta (Si/Ti = 35) after repeated reaction for eight and two times, respectively. (Inset: the magnified spectrum of Ti-YNU-1.)

runs, showing that within eight runs, the cyclohexene conversion was between 31.5 and 34.5%, whereas epoxide selectivity was in the range 87.5–92.8%. This indicates that Ti-YNU-1 is a stable catalyst. In contrast, Ti-Beta led to a 23% reduction in cyclohexene conversion after three runs, which is consistent with our previous result that the activity of Ti-Beta for the oxidation of 2-cyclohexene-1-one was decreased by 34% on three successive uses with reactivation [8]. The decrease in Ti-Beta activity might be due to the irreversible change of the Ti state from the tetrahedral to octahedral coordination (Fig. 11b). This is in agreement with results reported by

Carati et al. [37]. In addition, the partial removal of titanium from the framework by the reaction with H_2O_2 and/or by the porous reaction product, such as polyols, may be other reasons for the loss of activity [37,38]. In contrast, Ti species other than tetrahedrally coordinated titanium were still absent in the Ti-YNU-1 even after eight successive reaction recycles, as evidenced by the diffuse reflectance spectroscopy in which there was only one band centered at about 210 nm (Fig. 11a).

4. Conclusion

A new titanosilicate molecular sieve, Ti-YNU-1, with the structure analogous to MWW-type lamellar precursors has been synthesized by an elaborate method. XRD characterization showed that the interlayer spacing was increased by about 2.5 Å compared with Ti-MWW materials. The formation of Ti-YNU-1 is highly dependent on the Si/Ti ratio and also may be related to the removal of most templating molecules by acid treatment. FTIR and ^{29}Si MAS NMR spectroscopies and H_2O adsorption experiments confirmed that more silanol groups are present in Ti-YNU-1 than in Ti-MWW. In addition, ^{29}Si MAS NMR spectroscopy also showed that the local environment of T species at T_1 sites is markedly different from that of Ti-MWW. The synthesis of Ti-YNU-1 requires keeping the Si/Ti ratio in the synthesis gel above 80 and washing the as-synthesized solids with acid under reflux conditions before calcination.

The catalytic test for the oxidation of different cycloalkenes over various titanosilicate molecular sieves and Ar adsorption indicated that the effective pore size of these materials increased in the order Ti-MWW < TS-1 < Ti-MOR < Ti-YNU-1 < Ti-Beta. Compared with the other titanosilicates, Ti-YNU-1 exhibited higher activity, selectivity, and stability in the liquid-phase epoxidation of bulky cycloalkenes with H_2O_2 as an oxidant. This shows that Ti-YNU-1 is a potential clean catalyst for the epoxidation of bulky organic substrates. The protic/aprotic nature and polarity of the solvents strongly influence the catalytic performance of Ti-YNU-1. Acetonitrile should be the solvent of choice in terms of both activity and selectivity.

Acknowledgments

W.F. gratefully thanks the Japan Society for Promotion of Science and the Japan Science and Technology Agency (JST) for a fellowship as a foreign researcher. This work was supported by the Core Research for Evolutional Science and Technology program of the JST.

References

[1] T. Taramasso, G. Perego, B. Notari, U.S. patent 441050, 1983.
[2] M.G. Clerici, G. Bellussi, U. Romano, J. Catal. 129 (1991) 159.
[3] G. Bellussi, M.S. Rigutto, Stud. Surf. Sci. Catal. 85 (1994) 177.
[4] P. Ratnasamy, D. Srinivas, H. Knözinger, Adv. Catal. 48 (2004) 1.
[5] B. Notari Adv. Catal. 41 (1996) 253.
[6] M.G. Clerici, P. Ingallina, J. Catal. 140 (1993) 71.
[7] A. Corma, M.A. Camblor, P. Esteve, A. Martínez, J. Pérez-Pariente, J. Catal. 145 (1994) 151.
[8] M. Sasidharan, P. Wu, T. Tatsumi, J. Catal. 205 (2002) 332.
[9] Y. Goa, P. Wu, T. Tatsumi, Chem. Commun. (2001) 1714.
[10] Y. Goa, P. Wu, T. Tatsumi, J. Phys. Chem. B 108 (2004) 8401.
[11] A. Corma, V. Fornes, S.B. Pergher, Th.L.M. Maesen, J.G. Buglass, Nature 396 (1998) 353.
[12] A. Corma, U. Diaz, V. Fornes, J.L. Jorda, M. Domine, F. Rey, Chem. Commun. (1999) 779.
[13] M.E. Leonowicz, J.A. Lawton, S.L. Lawton, M.K. Rubin, Science 264 (1994) 1910.
[14] J.C. Cheng, T.F. Degnan, J.S. Beck, Y.Y. Huang, M. Kalyanaraman, J.A. Kowalski, C.A. Loehr, D.N. Mazzone, Stud. Surf. Sci. Catal. 121 (1999) 53.
[15] P. Wu, T. Tatsumi, T. Komatsu, T. Yashima, J. Catal. 202 (2001) 245.
[16] P. Wu, T. Tatsumi, J. Phys. Chem. B 106 (2002) 748.
[17] P. Wu, T. Tatsumi, Chem. Commun. (2002) 1026.
[18] W. Fan, P. Wu, S. Namba, T. Tatsumi, Angew. Chem. Int. Ed. 43 (2004) 236.
[19] G.J. Kennedy, S.L. Lawton, M.K. Rubin, J. Am. Chem. Soc. 116 (1994) 11000.
[20] M.A. Camblor, C. Corell, A. Corma, M. Díaz-Cabañas, S. Nicolopoulos, J.M. González-Calbet, M. Vallet-Regí, Chem. Mater. 8 (1996) 2415.
[21] J. Ruan, P. Wu, B. Slater, O. Terasaki, Angew. Chem. Int. Ed. 44 (2005) 6719.
[22] A. Clearfield, M. Kuchenmeister, J. Wang, K. Wade, Stud. Surf. Sci. Catal. 69 (1991) 485.
[23] M. Kurian, S. Sugunan, Micropor. Mesopor. Mater. 83 (2005) 25.
[24] W. Fan, R. Duan, R. Ohnuma, Y. Kubota, T. Tatsumi, in preparation.
[25] H.G. Karge, J. Weitkamp (Eds.), Characterization I, Molecular Sieves Science and Technology, vol. 4, Springer-Verlag, Berlin, 2004, p. 96.
[26] G.P. Heitmann, G. Dahlhoff, W.F. Hölderich, J. Catal. 186 (1999) 12.
[27] M. Hunger, S. Ernst, J. Weitkamp, Zeolites 15 (1995) 188.
[28] G. Engelhardt, R. Radeglia, Chem. Phys. Lett. 108 (1984) 271.
[29] P. Wu, T. Tatsumi, T. Komatsu, T. Yashima, Chem. Lett. (2000) 774.
[30] P. Wu, W. Fan, T. Tatsumi, in preparation.
[31] T. Maschmeyer, F. Rey, G. Sanker, J.M. Thomas, Nature 278 (1995) 159.
[32] Ch. Baerlocher, W.M. Meier, D.H. Olson, Atlas of Zeolite Framework Types, Elsevier, Amsterdam, 2001, pp. 77, 191, 203.
[33] M.G. Clerici, Top. Catal. 15 (2001) 257.
[34] A. Corma, P. Esteve, A. Martínez, J. Catal. 161 (1996) 11.
[35] G. Bellussi, A. Carati, M.G. Clerici, G. Maddinelli, R. Millini, J. Catal. 133 (1992) 220.
[36] N. Jappar, Q. Xia, T. Tatsumi, J. Catal. 180 (1998) 132.
[37] A. Carati, C. Flego, E. Previde-Massara, R. Millini, L. Carluccio, W.O. Parker Jr., G. Bellussi, Micropor. Mesopor. Mater. 39 (1999) 137.
[38] L.J. Davis, P. McMorn, D. Bethell, P.C. Bulman Page, F. King, F.E. Hancock, G.J. Hutchings, J. Mol. Catal. A Chem. 165 (2001) 243.